Polystyrene Nanoparticles with Anionically Polymerized Polybutadiene Brushes

Lei Zheng,* Anne Feng Xie, and John T. Lean

The Goodyear Tire & Rubber Company, 1485 East Archwood Avenue, Akron, Ohio 44306

Received July 22, 2004; Revised Manuscript Received September 7, 2004

ABSTRACT: Model hairy nanoparticles of highly cross-linked polystyrene (PS) cores and linear polybutadiene (PBd) brushes were synthesized. The PS cores were obtained using conventional microemulsion polymerization. The linear PBd brushes were synthesized using surface initiated living anionic polymerization. The PS core nanoparticles of 44 ± 12 nm in diameter (volume weight average) were first lithinated using a combination of butyllithium and *N,N,N′,N′*-tetramethylethylenediamine. Butadiene was subsequently polymerized at the surface of the particles. Two series of samples were synthesized with different degrees of polymerization (N) and grafting densities (σ). In the first series, while σ was constant at ∼0.14 chains/nm^2 (∼500 chains per particle), N changed from 37, 74, 139, to 198. Accordingly, the M_w of brushes changed from 2.0, 4.0, 7.5, to 10.7 kg/mol. In the second series, the weight ratio between PS and PBd was fixed at PS/PBd ≅ 5/2 (σN was constant in this case) and σ varied from 0.15 to 0.08 chains/nm^2 and lower. On the basis of the atomic force microscope (AFM) results, it was found that these hairy particles appeared to obtain better dispersion in PBd matrix as N of grafted chains was increased in the first series. More pronounced changes were observed, such as severe aggregation of particles, when σ decreased from relatively high to low with fixed total weight of brushes in the second series. The results were explained using theoretical calculations for grafted planes in contact with a chemically identical melt. In the system of grafted particles with short brushes ($N < P$, P is the degree of polymerization of the melt) studied in this paper, it was realized that the parameter $\sigma\sqrt{N}$ can represent the surface characteristics of the particles and be correlated to the dispersion of particles. A higher $\sigma\sqrt{N}$ value corresponds to better dispersion. The properties of cured rubber samples containing hairy particles were also examined using a rubber process analyzer (RPA) and a dynamic mechanical analyzer (DMA). RPA results are consistent with the morphological changes observed with AFM in terms of the "Payne effect". DMA results show that the glass transition temperatures, associated with the core and brushes, shift when the morphology changes. The AFM, RPA, and DMA results prove the strong correlation among the nanostructure of brushes, the microscopic dispersion of particles, and macroscopic properties of nanocomposites.

Introduction

Nanoparticles with brushes or "hairy" nanoparticles, where linear polymer chains are covalently attached to the surface of the core particles, can offer novel properties associated with nanometer sized particle cores and compatibility with their environment due to the brushes. A few examples are silica nanoparticles[1−3] and gold nanoparticles[4] with polymer brushes. A great deal of attention has been drawn to these hairy particles recently, partially due to great interest and expectations for nanocomposites. A nanocomposite typically refers to a matrix containing discontinuous particles having one major dimension on the length scale of 1−100 nm. The use of hairy particles is considered to be a general strategy to functionalize or compatablize the surface of the nanoparticles and to manipulate the interaction between particles and matrix. Despite great strides in synthesis and characterization of nanoparticles, there is limited knowledge in the literature on the properties of nanocomposites. Questions on the correlation among the morphology of brushes, the morphology of composites, and mechanical properties of composites have not been addressed in detail. In this paper, we plan to answer some of the questions by examining a model polystyrene (PS) nanoparticle with polybutadiene (PBd) brushes. The major focus of our study was the influence of brush structural changes on the dispersion of nanoparticles as well as the rheological properties associated with nanocomposites. A systematic study on this subject will help to understand the significant surface effects of brushes on the mechanical properties of nanomaterials.

Traditional incorporation of particulate fillers, such as carbon black or silica, in rubber compositions to improve mechanical properties is well-known, especially in the tire and rubber industry. There have also been some common interests in the use of rigid emulsion particles, specifically PS nanoparticles to reinforce rubbery materials. Early work from Kraus et al. reported on the properties of styrene−butadiene rubber reinforced by 40 nm polystyrene particles.[5] Morton examined similar systems.[6] Recently, Cai et al. reported that 315 nm cross-linked polystyrene particles in polysulfide rubber gave improved modulus, fracture strength, and elongation at break.[7] Nevertheless, in all the studies mentioned, there was limited control over the interfacial interactions between particle−particle and particle−matrix. The use of hairy particles is expected to provide better control over the interactions between particles and polymers in a composite material.

A variety of strategies have been explored for the synthesis of brushes on the surface of nanoparticles. To achieve controlled microstructure, such as molecular weight and grafting density, a living or controlled polymerization has to be applied to the surface. Ex-

* To whom correspondence should be addressed. Current address: Strategic Technologies, GlaxoSmithKline, 5 Moore Drive (2.3065), Research Triangle Park, NC 27709. E-mail: lei.x.zheng@gsk.com.

10.1021/ma048499v CCC: $27.50
Published on Web 11/25/2004

amples of surface-initiated polymerization techniques include anionic,[3,8−11] cationic,[12] controlled free radical polymerization,[13] and ring-opening metathesis polymerization.[14] Among these different methods, anionic polymerization is the best to control the microstructures of polymer chains and to polymerize diene type monomers, such as butadiene and isoprene.[15] Anionic polymerization can provide a variety of well-defined microstructures with precise molecular weight, molecular weight distribution, different architectures[16] and, more importantly, the control of 1,2-/1,4- and cis/trans contents for diene polymerization. The drawback of anionic polymerization is that it requires high-purity solvent and reagents as well as an inert atmosphere. As the most versatile polymerization technique, it has been used to grow polymer brushes from particles of silica gel,[11] graphite and carbon black,[17] clays,[10] and silica nanoparticles.[3] Since we were particularly interested in a surface layer of elastomeric polymer grafted from polystyrene nanoparticles and its control over dispersion in a rubbery matrix, lithium-initiated living anionic polymerization was chosen to generate brushes in this study.

A system containing hairy particles and a matrix polymer is comprised of three components: the core particles, the brushes, and the matrix. The covalently attached brushes are essentially an interphase between the particles and polymer matrix. Theoretical work on the interface between a polymer brush and a bulk melt of chemically identical chains dates back to the 1980s, when de Gennes introduced a detailed description of the conformation of polymer chains grafted onto a planar surface.[18] In his work, a scaling law was applied to elucidate the conformations and the concentration profiles for grafted chains in contact with a melt of the same polymer with shorter chains ($N > P$, N is the degree of polymerization of brush polymers and P is the degree of polymerization of matrix polymers). Later work considered the penetration length of free polymer into the grafted layer, λ, described by scaling laws, for cases of both $P > N$ and $N < P$.[19−21] A detailed study of polymer brushes on flat surfaces by Ferreira et al.[22] found a scaling criterion $\sigma\sqrt{N} > (N/P)^2$, which indicated that flat surfaces grafted with polymer brushes in a medium of long chain polymer melt could show attractive interactions between each other for sparsely grafted layers provided that P is large enough. The attractive interaction was credited to the positive surface tension between brushes and melt. Using mean-field calculations, Hasegawa et al.[23] studied the dispersion of hairy particles with diameters of hundreds of nanometers in a melt of long polymer chains. Their results showed an optimum grafting density for dispersion where the interaction potential of the brushes exhibited a very shallow attractive minimum. A theoretical model of hairy nanoparticles in the melt has not been fully developed to this point. Interestingly, Roan and Kawakatsu employed a new self-consistent-field (SCF) calculation in a closely related area involving hairy nanoparticles in good solvents. Their results pointed out that most previous theoretical studies dealt with either planar surfaces or large particles having small curvature.[24] Both structures are inadequate to explain the case when particle size is reduced to a level comparable with the size of the brushes. In this paper, a model nanoparticle of PS with PBd brushes in a PBd matrix was studied in terms of dispersion, rheological, and dynamic mechanical properties. The experimental results are interpreted with available theoretical predictions. The difference between our work and previous work[23,25,26] is that we examined the dispersion of nanoparticles with short chain brushes in a matrix of very long chains ($P \gg N$). In addition, we focused on the properties of a cross-linked rubbery matrix instead of a polymer melt containing these particles. The situation is more applicable to nanocomposite applications where short brushes are typically used.

Experimental Section

Preparation of Cross-Linked PS Core Particles. A glass quart bottle sealed with a rubber septum and Teflon liner was charged with a soap solution composed of 423.8 g of reverse osmosis (RO) water, 0.58 g of tripotassium phosphate, 65.3 g of a 10% solution of C14−18 unsaturated fatty acid potassium salt (Twin Rivers Technologies or Cognis), 5.4 g of a 20% solution of the potassium salt of disproportionated rosin acid (Arizona Chemical or Westvaco Specialty Chemicals), and 1.2 g of a 47.5% active dispersion of sodium naphthalenesulfonate−formaldehyde (Hampshire Chemical). The pH of the soap solution was adjusted to 10.5−11.0 with a 20% potassium hydroxide solution. To the bottle was added an activator solution composed of 10 g of RO water, 0.30 g of hydroxymethanesulfinic acid monosodium salt dihydrate (Royce Associates), and 0.09 g of sodium ferric ethylenediaminetetraacetate trihydrate (Hampshire Chemical). 181.8 g of styrene and 68.2 g of 55% divinylbenzene (Aldrich, 45% ethylvinylbenzene) were then added to the bottle, and the mixture was purged with nitrogen gas for 5 min to remove oxygen. The bottle was sealed and placed in a 10 °C water bath and rotated at 20 rpm. When the contents of the bottle reached bath temperature, 0.69 g of a 40% active pinane hydroperoxide (Millennium Specialty) was added. The reaction was allowed to proceed until the solids content reached a plateau of 30% solids. The particle size was determined by light scattering and fit to a Gaussian distribution (submicron particle sizer, NICOMP 370, particle sizing systems). The particle sizes determined were intensity weight-average 55 ± 15 nm, volume weight average 44 ± 12 nm, and number weight average 34 ± 10 nm.

The coagulation and isolation of the polymer particles were performed by adding 15 g of NaCl to ∼2 kg of RO water. The pH of the solution was lowered to between 3 and 4 with an 18% sulfuric acid solution. The latex was slowly added to the coagulation solution under rapid stirring. During the addition of latex, the pH was maintained between 3 and 4. After coagulation the polymer was washed three times with RO water and placed in a 65 °C oven with circulating air to dry. When the moisture level was below 1%, the particles were washed again in a filter with copious amount of acetone to remove residual water and surfactant. The particles were further dried under vacuum at 70 °C overnight.

Preparation of PBd Brushes on PS Particles. 50.0 g of dry polystyrene cores and 500 mL of dry hexanes were charged to a glass quart bottle. The suspended solution was sonicated for 30 min using a 600 W sonicator with a 10 in. wave extender. Sonication was used to break apart the aggregates of polystyrene particles. The suspended solution was then purged with nitrogen for about 30 min and sealed with a rubber septum and Teflon liner. To the bottle 10 mL of 1.6 M *n*-butyllithium hexane solution and 1.0 mL of *N,N,N′,N′*-tetramethylethylenediamine (TMEDA) were injected through the septum. The sealed bottle was placed in a 65 °C water bath and rotated at 20 rpm for 30 min. The lithiated PS particles showed dark orange color. Butadiene in hexanes (∼15 wt %) was then introduced, and the color changed to yellow. The bottle continued to be heated in the water bath to the full conversion of butadiene (typically 2−3 h). The reaction was stopped by injection of 2-propanol, and 1% butylated hydroxytoluene (BHT) was added. A small sample was taken for AFM imaging if necessary. The particles were dried in the hood until constant weight.

The molecular weight of the brushes was determined on residual homopolymers extracted using hexanes. GPC was performed in THF using a Wyatt light scattering detector, and a d*n*/d*c* value of 0.120 was used to calculate the molecular weight.

Preparation of the Compound Mixture. Mixing of the particles and polymers was accomplished in two stages: nonproductive and productive. The first stage (nonproductive) involved adding half of the particles and polymers mixture to a 55 cm^3 Haake Rheomix 90 equipped with a throat, with all the temperature control zones set at 145 °C and rotors at a mixing rate of 50 rpm. After the first half of the mixture was added to the mixer, the other ingredients of the nonproductive were added. As soon as the nonproductive ingredients were added, the rest of the particles and polymers mixture was added in order to clear the throat of any remaining material. The ram was lowered, and the material was mixed for 6.0 min, ensuring that the temperature did not exceed 170 °C. The final mixture of nonproductive contained 100 phr (parts per hundred parts of rubber, by weight) rubbery polymer PBd, including matrix and brushes, 60 phr filler PS cores, 2 phr stearic acid, and 3 phr zinc oxide.

The productive mix was run under the same conditions, except that the temperature zones of the mixer were controlled at 100 °C. One-half of the mixed nonproductive material was added to the mixer followed by the productive ingredients (0.9 phr *N-tert*-butylbenzothiazole-2-sulfenamine (TBBS) and 1.5 phr sulfur) and the second half of the nonproductive. The ram was lowered, and the material was mixed for 3 min with the temperature not to exceed 115 °C.

After the productive mix was completed, the samples were passed six times endwise through a mill set at 0.032 in. in order to create a sheet for testing.

Atomic Force Microscope (AFM). AFM experiments were carried out with a Multimode Nanoscope III (Digital Instruments) scanning probe microscope equipped with phase detection electronics. Images were acquired in the tapping mode under ambient conditions. The commercial silicon (Si) cantilever oscillation frequency was 250 Hz. Both height and phase images were recorded simultaneously at the intrinsic resonance frequency of the cantilever. For a typical 7.5 μm scan size, images were collected with a scan rate of 1 Hz and a resolution of 512 samples per line. To obtain images of free particles in solution, samples were taken at the end of the polymerization and further diluted with hexanes to ca. 0.1 wt % and then deposited onto a silica wafer. To obtain images of hairy particles in rubber compound, particles with PBd brushes and matrix PBd were mixed with the mixing protocol described above. After the samples were cured, they were cryomicrotomed at −80 °C to a thickness of 4 μm.

Rubber Process Analyzer (RPA). The compounds were milled to provide a sheet of the material. Approximately 5 g of the compound was cut from the sheet. The data were collected on RPA 2000 using a standard test method. The test method was divided up into four subtests. The first subtest was conducted at 100 °C with a 2% strain deformation and at 0.333 and 3.33 Hz. The second subtest was also made at 100 °C and employed a 15% strain at 0.833 and 8.33 Hz. The third subtest was a cure at 191 °C for a run time of 4.88 min. The cure curve was generated for a strain of 3.5% at a frequency of 1.667 Hz. Subtest 4 was a strain sweep (1.0%, 5.0%, 10.0%, 30.0%, and 50.0%) at 100 °C and 1.0 Hz. G' vs strain data from subtest 4 were plotted and analyzed.

Dynamic Mechanical Thermal Analyzer (DMA). Dynamic mechanical thermal analysis was collected on a Rheometric Scientific solid analyzer RSA II running in tensile mode at an oscillation frequency of 1 Hz. Rectangular samples were used with approximate length of 20 mm, width of 6.4 mm, and thickness of 0.5 mm. The strain amplitude was set to 0.1% strain, well within the linear viscoelastic range. A gaseous nitrogen purge and a heating rate of 5 °C/min were used.

Results and Discussion

Synthesis of Hairy Nanoparticles. The PS core particles were synthesized using conventional microemulsion polymerization. A standard emulsion polymerization procedure was used with a redox initiator system and a mixture of fatty acid and rosin acid as surfactants. Microemulsion polymerization provides a convenient way to obtain spherical nanoparticles or microgels[27] in the range of 20−200 nm. In our study, the polystyrene particles have a volume weight average diameter of 44 nm and number average diameter of 34 nm ($D_w/D_n = 1.3$). In contrast to PS particles reported previously, the unique design in these particles was the introduction of high concentration of divinylbenzene (DVB). 15 wt % DVB (27.3 wt % 55/45 DVB and ethylvinylbenzene mixture) was copolymerized with styrene in the reaction bottle. The intention was to obtain particles that can be used at elevated operation temperature without deformation. The cross-linking of DVB increased the glass transition temperature of the particle. In addition, a highly cross-linked PS particle should maintain its shape and integrity even above its glass transition temperature. One point worth mentioning here is that the approach to use styrene−butadiene block copolymer micelles[28] PS-*b*-PBd or star block copolymer of PS-*b*-PBd coupled with DVB[29] to form phase-separated PS domains would not be feasible for the application where discrete spherical particles are desired. It is because the mixing temperature to compound fillers and rubbers is typically around 150 °C, well above the T_g of PS (around 100 °C). As a result, the shape and size of PS domain will change after mixing and may not reinforce the rubber in a desirable way. The use of DVB also had another function in our design. The different reactivity between the two vinyl groups in DVB produces some unreacted vinyl groups residing in the PS particles after polymerization. These vinyl groups can be used subsequently for functionalization and graft polymerization.[30]

Scheme 1. Synthesis of PS Nanoparticle with PBd Brushes

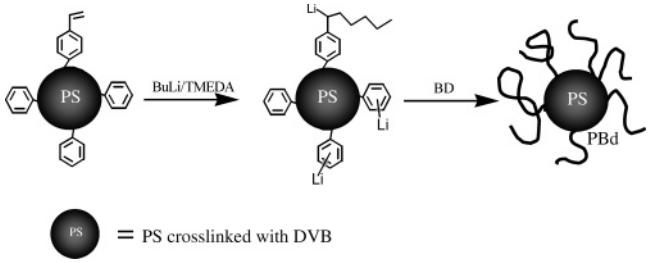

The reaction scheme is shown in Scheme 1 for surface-initiated living polymerization of butadiene from PS nanoparticles. It was carried out in two steps. *n*-Butyllithium (BuLi) was added to the suspended PS particles in hexanes in the first step. Combined with TMEDA, it can deprotonate the proton at the benzylic position of the benzene or any of the five hydrogens on the benzene.[31] The BuLi can also react with the unreacted vinyl groups of DVB. The next step involved the injection of butadiene monomers in hexanes and polymerization at 65 °C to obtain PBd brushes. Since PS is not soluble in hexanes, it is assumed that most of the lithination was at the surface of particles. At the end of polymerization, the free polymers initiated from free BuLi in solution were separated from hairy particles by hexane extraction and centrifuge. All the polymerization conditions and grafting efficiencies are listed in Table 1. The grafting efficiency of BuLi was determined on the basis of the weight ratio between brushes and total amount of PBd (brushes plus free polymers). When

Table 1. Polymerization Conditions and Molecular Weight Data

		initiation				molecular weight[b]	
entry	PS particles[a] (g)	BuLi (1.3 M, mL)	TMEDA (6.63 M, mL)	PBd brushes (g)	grafting efficiency (%)	M_w (kg/mol)	M_w/M_n
1	50.0	10.0	1.0	4	86	2.0	1.11
2	50.0	10.0	1.0	8	82	4.0	1.08
3	50.0	10.0	1.0	14	82	7.5	1.06
4	50.0	10.0	1.0	23	85	10.7	1.04
5	50.0	6.0	0.6	21	95	18.0	1.06
6	50.0	4.0	0.4	23	99		

[a] Reaction conditions: 50.0 g of PS in 500 mL of hexanes, 65 °C. [b] Molecular weight of brushes was estimated from free polymers in solution.

TMEDA was used, the grafting efficiencies were higher than 80% in all the cases (Table 1). They also depended on the amount of BuLi used. When a lesser amount of BuLi was injected, the free BuLi was significantly reduced (entries 5 and 6 vs 1−4). If TMEDA was not used, the efficiency was only a few percent simply due to limited amount of free vinyl groups on the surface. Without chelating ligands, such as TMEDA, BuLi cannot deprotonate PS.

The molecular weight of the brushes was estimated from free polymers based on the assumption that the polymerization kinetics was similar for bound and free lithium. Please note that the deprotonation of PS yields three different types of initiation sites (2° benzylic, 3° benzylic, and phenyl) while the initiation of free chains is a 1° alkyl chains. This should have some effect on the initiation efficiencies and rates and resulted in relatively broader polydispersity for bound polymers. Nevertheless, the molecular weight of brushes should be similar to the free polymers. The previous study on surface-initiated living anionic polymerization on silica nanoparticles showed the similar molecular weight and slightly broader molecular weight distribution for bound polymers compared with free polymers.[3] In our study, no convenient method was available to determine the molecular weight of brushes, and thus the molecular weight of free polymers was used as molecular weight indicators of the grafted brushes.

In the first step of reaction, extra amount of BuLi was used to scavenge residual water and surfactant. The remaining fragments of initiators from emulsion polymerization and some impurities (typically 3 ppm) in hexanes could also react with BuLi. It was realized during drying of the PS nanoparticles that the residual water or impurities were extremely difficult to remove below the 0.1% level, which was credited to the enormous amount of surface area of the PS particles allowing water and/or surfactant to be absorbed. Instead of a tedious procedure to clean the particles, an excess BuLi was used in this case.

In Table 1, entries 1−4 were designed to produce PS−PBd nanoparticles with the same grafting density but different molecular weight. By changing the amount of butadiene and fixing the amount of BuLi and TMEDA, a series of particles were prepared with the brush molecular weights around 2.0, 4.0, 7.5, and 10.7 kg/mol. The second set of samples, entries 4−6, were intended to produce hairy particles with the same total weight of brushes and different grafting densities. Consequently, the molecular weight also changed inversely with grafting density. Higher molecular weight associated with lower grafting density. In entry 6, the grafting efficiency was so high that no free polymer was extracted out using hexanes. In other words, all the BuLi was reacted with either PS particles or impurities. As a result, no molecular weight data are available for this entry.

To prove that we truly have produced nanoparticles with PS core and PBd brushes, a sample of hairy particles in hexanes was tested with AFM imaging analysis. The sample was taken at the end of the polymerization and further diluted with hexanes to around 0.1 wt %. It was deposited onto a silica wafer. To better image the brushes, the PS to PBd weight ratio was 1:2 for this test. The image is shown in Figure 1. Since PS is a high-T_g resin, it is shown as bright, round spheres in the center. While T_g of PBd is lower than room temperature, it surrounds PS particles as a soft corona. The PBd also spreads out on the substrate due to its high mobility. This spread-out resulted in the apparent larger surface area of brushes in the image and more importantly the visibility of PS cores.

Dispersion of Nanoparticles in Polybutadiene. The synthesized hairy particles in entries 1−6 were mixed in a Banbury mixer with PBd matrix polymer (Goodyear Chemical Budene 1209). The matrix polymers were synthesized using BuLi as initiator in a continuous polymerization process. The polymer has a weight-average molecular weight of 320 kg/mol (P = 5900) and polydispersity of 1.6. The mixing was completed in a Banbury in two steps with a standard sulfur cure package for PBd. After the samples were cured at 170 °C for the appropriate amount of time, they were cryo-microtomed at −80 °C to a thickness of 4 μm, and the cross sections were imaged using the Digital Instruments Multimode SPM with a TESP tip. The images are shown in Figures 2 and 3.

In a system of hairy particles with chemically identical brushes and matrix (χ = 0 in the Flory−Huggins notation), one needs to mainly deal with three parameters: N, the degree of polymerization of the brushes; P, the degree of polymerization of the matrix polymer; and σ, the grafting density of the brushes as the number of chains per unit monomer area. As mentioned in the synthesis section, we systematically varied N and σ while maintaining P constant.

In the first set of samples (entries 1−4, Table 1), as the weight-average molecular weight (M_w) or N gradually increased, so did the dispersion of the hairy particles in the rubber matrix. Figure 2 shows the AFM images for this series. The grafting densities were all 0.14 chains/nm^2 (~500 chains per particle). For the samples containing particles grafted with short chain brushes (M_w = 2.0, 4.0, and 7.5 kg/mol) (Figure 2a−c), mixtures of hairy particles and PBd matrix chains show regions with aggregates of particles. As the chain length of grafted brushes further increased (M_w = 10.7 kg/mol), particle aggregation was suppressed, resulting in rela-

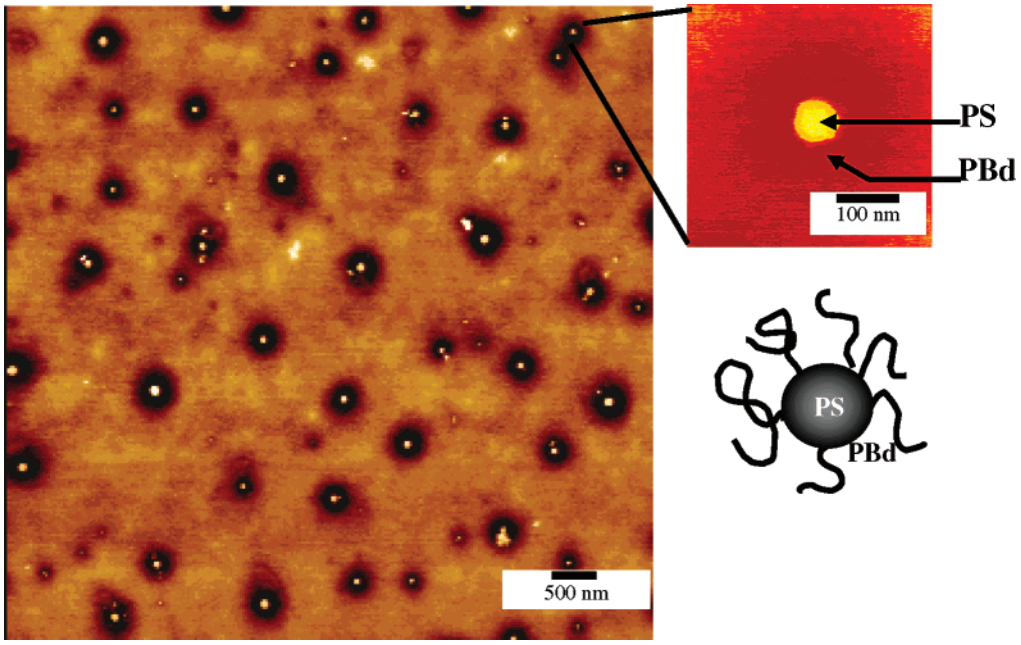

Figure 1. AFM images of hairy particles of PS core−PBd brushes (PS/PBd = 1/2).

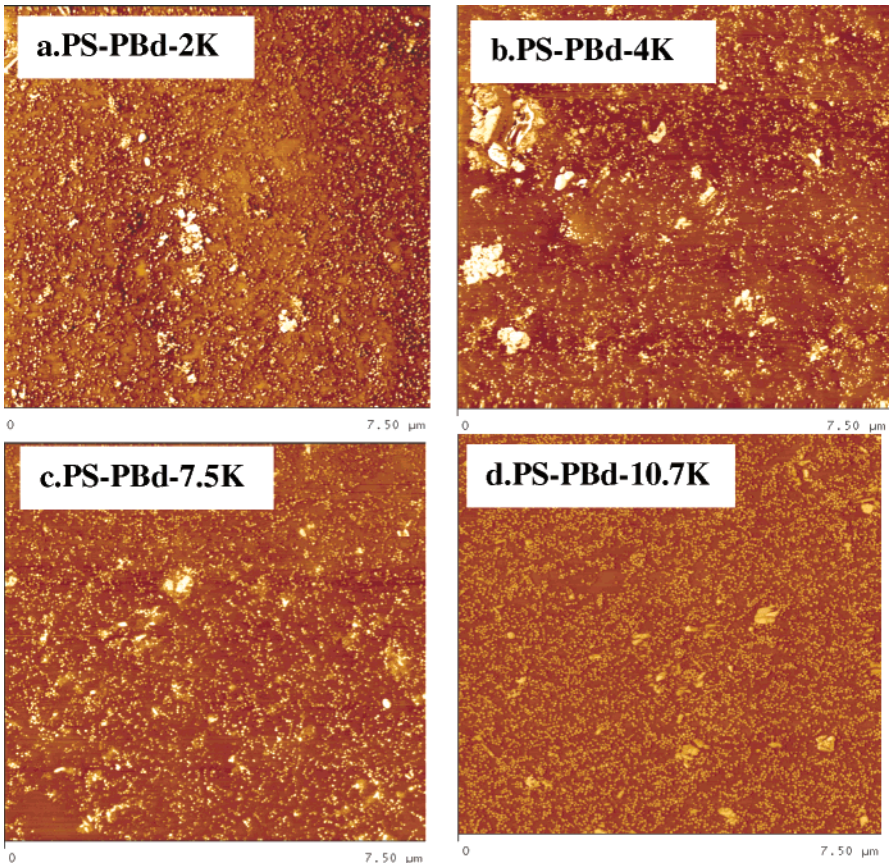

Figure 2. AFM images of hairy particles of PS core and PBd brushes in polybutadiene: Molecular weight effect on the dispersion or aggregation of the particles.

tively homogeneous particle distribution (Figure 2d). Hairy particles appeared to obtain better dispersion in PBd matrix when N of grafted chains was increased. Note that these samples were vulcanized rubber compounds containing about 3 wt % curatives (steric acid and zinc oxide), which contributed to occasionally visible, big, bright chunks in the AFM images.

As mentioned above, using the anionic polymerization method, we varied not only molecular weight but also grafting density of the brushes on particles. Our results showed that grafting density had a much more dramatic effect on the dispersion of the particles in the polymer matrix. In the second set of samples (entries 4−6, Table 1), the total weight of PBd brushes (σN) on particle surfaces was maintained the same, and the grafting density was changed from high to low. A series of AFM images are shown in Figure 3. With the amount of grafted brushes kept constant (PS/PBd $\cong$ 5/2), the

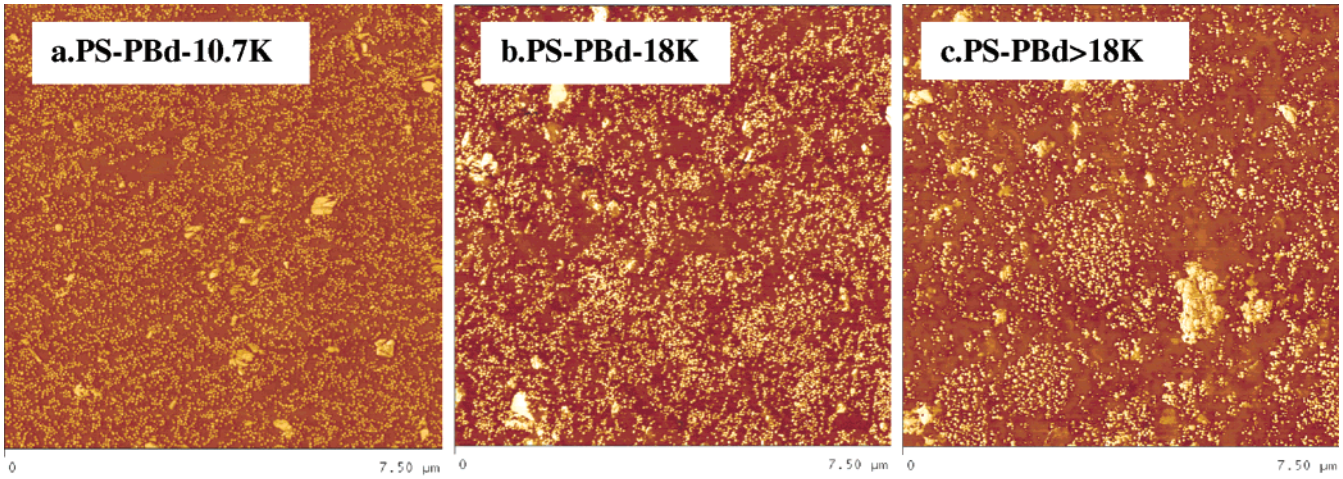

Figure 3. AFM images of hairy particles of PS core and PBd brushes in PBd matrix: grafting density effect on the dispersion or aggregation of the particles.

Table 2. Characteristics of PBd Brushes

entry	M_w of brushes (kg/mol)	repeat unit N	grafting density σ' (no. of chain/nm^2)[a]	$\sigma = \sigma' a^2$ (no. of chain/unit monomer area)[b]	$\sigma\sqrt{N}$
1. PS-PBd-2K	2.0	37	0.14	0.035	0.21
2. PS-PBd-4K	4.0	74	0.14	0.035	0.30
3. PS-PBd-7.5K	7.5	139	0.13	0.033	0.38
4. PS-PBd-10.7K	10.7	198	0.15	0.038	0.53
5. PS-PBd-18K	18.0	333	0.08	0.020	0.36
6. PS-PBd->18K		>333	<0.08	<0.020	<0.36

[a] Calculation of σ' was based on the equation provided in ref 23. [b] The butadiene monomer size a of 0.5 nm was used for calculation.

grafting density of the particles was decreased as the molecular weight of the brushes was varied from 10.7 to 18 kg/mol and to even higher. At the same time, the particle distribution in PBd matrix underwent a pronounced change from the well-dispersed system (Figure 3a) to slight aggregates (Figure 3b), to severe, large aggregates (Figure 3c).

In Table 2, we calculated N, σ, and $\sigma\sqrt{N}$ for systems in this study. Note that the σ' referred to is the grafting density in unit area (nm^2), and it should be normalized by monomer size for comparison between different polymers. One approach to obtain the solution to this system is self-consistent-field (SCF) calculation of the free energy between particles. The study by Hasegawa et al.[23] reported optimum grafting density for a dispersion of polymer-grafted particles suspended in a polymer matrix. They considered two major terms for interactions between two brushes in contact with the polymer melt. Between particles, there is always a van der Waals attraction, showing a steep negative (attraction) interaction potential at small separation distance. When the grafting density is very low, the van der Waals attraction is balanced by a repulsive interaction originating from the excluded-volume effect. The more polymers grafted on the surface, the longer range the repulsion is. Under these circumstances, the depth of attraction minimum becomes smaller with the increase in grafting density. On the other hand, their mean-field calculation presents an attractive part in polymer−polymer interaction if the grafting density becomes very high. The origin of this attraction is said to be surface tension. The increase of particle dispersion results in the increase of free energy due to surface tension between particles and matrix. Hence, the interaction potential of the brushes exhibits a very shallow attractive minimum at an intermediate grafting density. The conclusion was drawn that there exists an optimum grafting density for the dispersion of particles in polymer melt. Furthermore, their prediction gave an optimum grafting density of 0.1 when the degree of polymerization of both N and P were 100. They extended this value to the criterion to determine the brush regime—$\sigma' a^2\sqrt{N} \cong 1$, where a is the monomer size, consistent with the normalized grafting density mentioned above.

On the basis of the discussion above, the molecular weight effect on dispersion in Figure 2 is interpreted in the following ways. There was an entropic balance between the entropy of particles and the conformational entropy of matrix chains.[26] On one hand, the dispersion of particles in the matrix increased the entropy of particles. On the other hand, the dispersion required the matrix chains to diffuse into the close vicinity of hard-core spheres, where the conformation of free matrix chains was reduced. The aggregation of particles decreased this unfavorable volume zone around hard particles through overlapping of particles and therefore increased the free volume in the matrix. In our case the unfavorable volume zone was reduced when the molecular weight of brushes increased for entries 1−4, Tables 1 and 2. As a result, better dispersion was achieved with higher N values. Another way to understand our results is based on the free energy consideration. The attraction between particles due to van der Waals forces was balanced by the repulsion from excluded volume of brushes. At the same grafting density the higher the molecular weight of brushes was, the more brush volume existed at the surface of particles. Thus, the repulsion between particles increased as the molecular weight went up, which introduced better dispersion.

An interesting question raised during our study was whether the dispersion can be correlated to the total weight of brushes (σN). Previous limited studies indicated for coated particles increasing either σ or N would increase the dispersion.[23,26] One can therefore argue

that the total weight of brushes is the controlling factor since more brushes on the surface of particles would increase the compatibility between the particles and the matrix. To answer this question, the second set of experiments were designed to maintain the total weight of brushes grafted (σN) constant and decrease the grafting density. As shown in Table 2, entries 4−6, the decrease in grafting density (σ) was accompanied by an increase in molecular weight. Our AFM results in Figure 3 showed a significant difference in morphology with the decrease in grafting density despite a fixed σN. Because the thickness or the height of the repulsion layer goes with $\sigma\sqrt{N}$, we compare the term $\sigma\sqrt{N}$ for all cases in Table 2. There is an obvious trend that the dispersion of particles in PBd matrix is consistent with the value of $\sigma\sqrt{N}$, which includes both grafting density and molecular weight factors. Particle dispersion was improved accompanied by the increase of $\sigma\sqrt{N}$ from entries 1 to 4, while aggregation occurred and cluster size increased as $\sigma\sqrt{N}$ decreased from entries 4 to 6. (We were unable to determine the molecular weight of entry 6 but assumed its $\sigma\sqrt{N}$ value should be much lower than that of entry 5.) Specifically in the second set of data the thickness of the repulsion layer decreased as the grafting density dropped, reflected by increasing depth of attraction minimum from free energy considerations. The molecular weight increase, inversely to the grafting density, went with the square root of N and could not compensate for the repulsion loss due to the grafting density's drop. Consequently, the dispersion of grafted particles in PBd matrix became worse.

Rheological Properties of Nanocomposites. A strong correlation between the dispersion of the particle fillers and rheological properties was discovered when dynamic moduli were measured as a function of strain on a series of vulcanized samples presented above. Shown in Figure 4 is a plot of storage modulus measured at 100 °C and 1 Hz vs the logarithm of strain amplitude obtained from RPA. For unfilled compound, the moduli showed little or no change with the increase of strain amplitude over the test range. In contrast, the moduli of filled compounds decreased upon increasing strain, showing the typical nonlinear behavior known as the "Payne effect".[32,33] Though the mechanism for reinforcement and nonlinearity remains controversial, it has been widely accepted that the Payne effect is related with filler deagglomeration and breakdown of the filler network. It is believed that the Payne effect can serve as a measure of filler agglomeration and the network originated from filler−filler and polymer−filler interactions.[34] At small strain amplitude, the decrease of modulus stems from the breakdown of the filler network, which is dominated by filler−filler interactions, while at large strain amplitude, modulus further decreases as a result of detachment of polymer and filler, determined by polymer−filler interactions. In Figure 4a, the Payne effect becomes less upon increasing the molecular weight of grafted chains, indicating a lower degree of filler agglomeration and better dispersion for particles with longer brushes. We also investigated the effect of grafting density, shown in Figure 4b. It was found that when the grafting density was decreased, the Payne effect became more significant, suggesting a higher degree of filler agglomeration. It is considered that filler particles and the polymer matrix experienced substantial entanglement. The longer the free chains can penetrate into brushes, the more entanglement we expect between filler particles and the polymer matrix. The degree of entanglement can be reflected by the modulus measurement at large strain amplitude. For brushes with molecular weight below 10.7K, the highest applied strain amplitude was adequate to disrupt the entanglement between polymer matrix and hairy particles. Therefore, the values of G' showed no difference at 50% strain for particles with brushes no longer than 10.7K. Nevertheless, if the molecular weight of brushes exceeded 10.7K, 50% applied strain was not sufficient to break polymer and filler interactions due to strong entanglement. As a consequence, the modulus at 50% strain remained higher for particles with longer brushes. The results demonstrated the potential to control rheological properties by tailoring the nanostructure at the surface of particles.

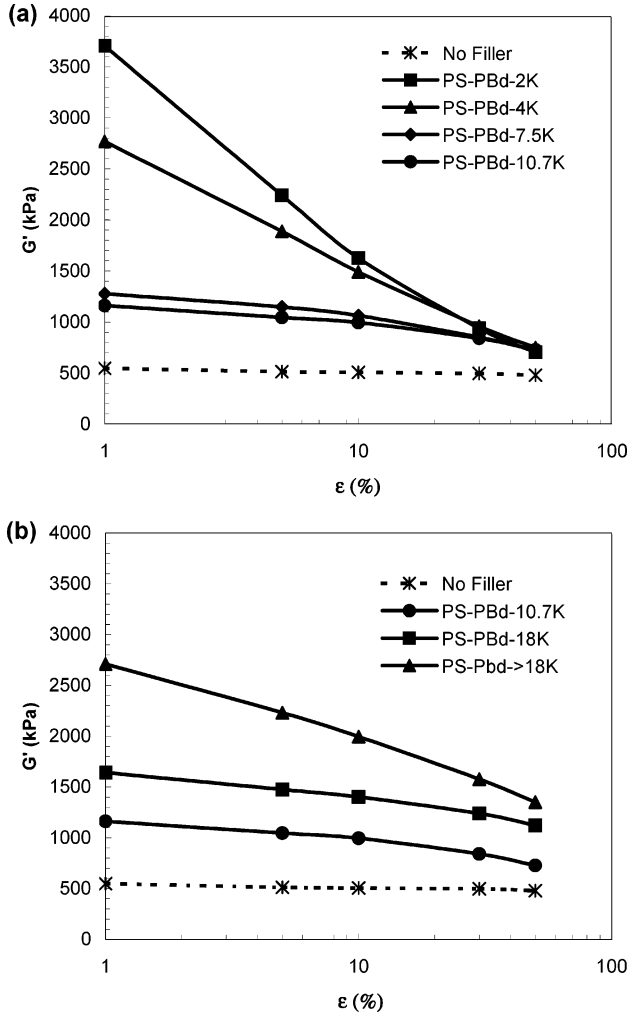

Figure 4. RPA results of hairy particles of PS core and PBd brushes in PBd matrix: molecular weight (top) and grafting density (bottom) influence on Payne effect.

Dynamic Mechanical Properties of Nanocomposites. To further study for morphology and property correlation, dynamic mechanical measurements were carried out to examine the viscoelastic response of vulcanized PBd compounds filled with grafted particles. Figure 5 presents the loss tangent, tan δ, at 1 Hz, as a function of temperature. Figure 5a renders the dynamic response of PBd filled with particles coated with grafted brushes with molecular weight below 10.7K (Tables 1 and 2, entries 1−4), where two noticeable loss peaks are observed for all the samples. The first loss peak at −80

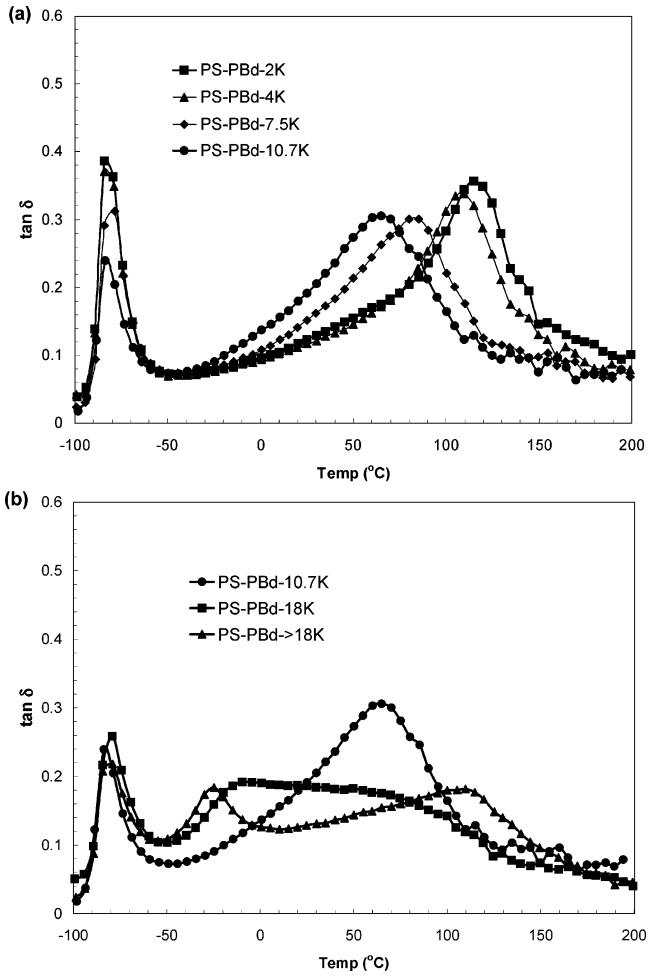

Figure 5. Dynamic mechanical properties of hairy particles of PS core and PBd brushes in PBd matrix: molecular weight (top) and grafting density (bottom) influence on tan δ.

°C represents the glass transition of the PBd matrix, while the second loss peak is at a much higher temperature range, representing the glass transition of hairy PS particles. The second loss peak above 0 °C undergoes a significant shift to lower temperatures with the increase of the molecular weight of grafted PBd chains. Since the precursor PS particles are highly cross-linked, it is difficult to determine the actual T_g using DSC measurements. Indirect measurements suggested that its T_g is higher than 150 °C. When embedded in a PBd matrix, the glass transition of the PS particles was lowered to 135 °C. This was caused by the partial compatibility of PS particles with the matrix. Moreover, when PS particles were coated with PBd brushes, the degree of particle softening by both PBd matrix and brushes becomes higher due to the increase of compatibility with the matrix. In this case, the computability of hairy particles and matrix with identical brushes and matrix chains is determined by the $\sigma\sqrt{N}$ value. As the molecular weights of the brushes were increased from 2.0K to 10.7K, the coated PS particles grew more compatible with the high molecular weight PBd matrix. As a result, the tan δ corresponding to the glass transition of particles in vulcanized compounds underwent a remarkable shift from 120 °C down to 70 °C. This was essentially similar to T_g softening of PS in a PBd-*b*-PS copolymer when the molecular weight of PBd was low and compatible with PS domains in the disordered regime.[35] An intriguing effect on the glass transition of coated particles was observed when both N and σ changed, shown in Figure 5b. We start with the extreme case where the molecular weight of the brush was very high (>18K). Three distinct loss peaks were noted in this case: one at −80 °C, the glass transition of PBd matrix; one at 110 °C, the glass transition of PS particles; and the third one showing up at −25 °C. This new peak was attributed to the glass transition of PBd brushes grafted on the particles. The much higher T_g of brushes was partially due to high vinyl concentration (1,2- addition instead of 1,4-) when TMEDA was used. Here the grafted brushes no longer presented a completely miscible phase with the core polymers once the molecular weight of the brushes increased to well above 18K. Consequently, the T_g of cross-linked PS cores recovered from 65 °C back to 110 °C, and a separate peak for the brush layer appeared. For the case when the molecular weight and grafting density is in the middle of series, the peaks of PS cores and PBd brushes became indistinguishable. Instead, an extremely broad tan δ spanning from −10 to 100 °C appeared, indicating that coated particles were at the edge of miscible/immiscible phase transition between the brushes and the cores in a matrix.

Conclusion

Model hairy nanoparticles of PS core and PBd brushes were synthesized using lithium-initiated living anionic polymerization. It was achieved by lithinating PS particles surface using combination of BuLi and TMEDA and subsequently polymerizing butadiene in hexanes. Two series of samples were synthesized with different degrees of polymerization (N) and grafting densities (σ). In the first series, while σ was constant at ∼0.14 chains/nm^2 (∼500 chains per particle), the N (M_w) changed from 37 (2.0K), 74 (4.0K), 139 (7.5K), to 198 (10.7K). In the second series, the total amount of brushes (σN) was fixed with PS/PBd ≅ 5/2 and σ varied from 0.038 to 0.020 chains/nm^2 and lower while N (M_w) varied from 198 (11K) to 333 (18K) and higher.

The parameters of N and σ were studied to examine the effect on the dispersion of hairy particles in a PBd matrix with very long chain polymers. On the basis of the AFM images, it was found out that these hairy particles appeared to obtain better dispersion when N of grafted chains was increased in the first set of experiments. More pronounced changes were observed with more aggregation of particles when σ changed from relatively high to low in the second series. The results were interpreted using theoretical predictions of brushed planes in contact with a chemically identical melt. The parameter of $\sigma\sqrt{N}$ was used to correlate to the dispersion. $\sigma\sqrt{N}$ essentially accounts for the surface coverage of the nanoparticle with brushes, taking account of both the grafting density and the radius of grafted chains. The higher the coverage is, the better the dispersion is.

The Payne effect was examined on the cured samples containing hairy particles. In the first series, when the molecular weight of brushes changed from 2.0K to 10.7K, a significant effect was observed. The shear storage moduli G' dropped significantly with strain amplitude increasing from 1% to 50%. In second series, when σ changed from 0.15 to 0.08 chains/nm^2 and lower while M_w (or N) increased, less Payne effect was noticed over the tested range of strain amplitude. A stronger filler−polymer interaction was observed at 50% strain

with higher G', possibly due to the length of brush chains exceeding minimal entanglement length.

Dynamic mechanical thermal analysis was also used to characterize the cured samples. It was found that the T_g of highly cross-linked PS core particles decreased from 120 to 70 °C when the M_w of brushes increased from 2.0K to 10.7K in the first series of samples. This observation is credited to the increased compatibility ($\sigma\sqrt{N}$) of the hairy particles with matrix when the molecular weight of brushes was fairly low and miscible with PS core. Interestingly, when the ratio of PS to PBd was fixed around 5/2 and σ decreased while N increased, the brushes became immiscible with the core. The T_g of hairy particles underwent from one peak around 70 °C, through a broad peak across −10 to 80 °C, to two peaks around −25 and 110 °C separately. The separation of peaks was explained on the basis of the phase separation between PS cores and PBd brushes when the M_w of brushes went above the critical value. The decreased compatibility of hairy particles and matrix contributed to the increased T_g of PS cores.

In summary, we have shown that the morphology of brushes based on σ and N has a significant impact on the dispersion of nanoparticles in the matrix. For grafted particles with short brushes, $\sigma\sqrt{N}$ appears to be a good indicator of brush morphology with higher value associated with better dispersion. As the dispersion changes, the rheological properties of the nanocomposites change accordingly. So do the dynamic properties of the composites. The results have shown that mechanical properties of nanocomposites are significantly affected by the brush morphology of hairy particles.

Acknowledgment. We thank Dr. Adel Halasa, Dr. Bill Hsu, and Dr. Jinping Zhou for the helpful discussion about anionic grafting reactions. We also thank Penny Gray for the assistance to obtain AFM images.

References and Notes

(1) von Werne, T.; Patten, T. E. *J. Am. Chem. Soc.* **2001**, *123*, 7497.
(2) Bartholome, C.; Beyou, E.; Bourgeat-Lami, E.; Chaumont, P.; Zydowicz, N. *Macromolecules* **2003**, *36*, 7946.
(3) Zhou, Q.; Wang, S.; Fan, X.; Advincula, R.; Mays, J. *Langmuir* **2002**, *18*, 3324.
(4) Ohno, K.; Koh, K.-m.; Tsujii, Y.; Fukuda, T. *Macromolecules* **2002**, *35*, 8989.
(5) Kraus, G.; Rollmann, K. W.; Gruver, J. T. *Macromolecules* **1970**, *3*, 92.
(6) Morton, M. In *Advances in Chemistry Series*; Platzer, N. A. J., Ed.; American Chemical Society: Washington, DC, 1971; Vol. 99, p 490.
(7) Cai, J. J.; Salovey, R. *J. Mater. Sci.* **1999**, *34*, 4719.
(8) Jordan, R.; Ulman, A.; Kang, J. F.; Rafailovich, M. H.; Sokolov, J. *J. Am. Chem. Soc.* **1999**, *121*, 1016.
(9) Quirk, R. P.; Mathers, R. T. *Polym. Bull. (Berlin)* **2001**, *45*, 471.
(10) Zhou, Q.; Fan, X.; Xia, C.; Mays, J.; Advincula, R. *Chem. Mater.* **2001**, *13*, 2465.
(11) Oosterling, M. L. C. M.; Sein, A.; Schouten, A. J. *Polymer* **1992**, *33*, 4393.
(12) Jordan, R.; West, N.; Ulman, A.; Chou, Y.-M.; Nuyken, O. *Macromolecules* **2001**, *34*, 1606.
(13) Pyun, J.; Kowalewski, T.; Matyjaszewski, K. *Macromol. Rapid Commun.* **2003**, *24*, 1043.
(14) Weck, M.; Jackiw, J. J.; Rossi, R. R.; Weiss, P. S.; Grubbs, R. H. *J. Am. Chem. Soc.* **1999**, *121*, 4088.
(15) Hsieh, H. L.; Quirk, R. P. *Anionic Polymerization*; Marcel Dekker: New York, 1996.
(16) Pitsikalis, M.; Pispas, S.; Mays, J. W.; Hadjichristidis, N. *Adv. Polym. Sci.* **1998**, *135*, 1.
(17) Tsubokawa, N.; Yoshinobu, T.; Sone, Y. *Colloid Polym. Sci.* **1991**, *269*, 324.
(18) de Gennes, P. G. *Macromolecules* **1980**, *13*, 1069.
(19) Witten, T. A.; Leibler, L.; Pincus, P. A. *Macromolecules* **1990**, *23*, 824.
(20) Zhulina, E. B.; Borisov, O. V.; Brombacher, L. *Macromolecules* **1991**, *24*, 4679.
(21) Gay, C. *Macromolecules* **1997**, *30*, 5939.
(22) Ferreira, P. G.; Ajdari, A.; Leibler, L. *Macromolecules* **1998**, *31*, 3994.
(23) Hasegawa, R.; Aoki, Y.; Doi, M. *Macromolecules* **1996**, *29*, 6656.
(24) Roan, J. R.; Kawakatsu, T. *J. Chem. Phys.* **2002**, *116*, 7295.
(25) Aoki, Y. *Macromolecules* **1987**, *20*, 2208.
(26) Lindenblatt, G.; Schärtl, W.; Pakula, T.; Schmidt, M. *Macromolecules* **2000**, *33*, 9340.
(27) Funke, W.; Okay, O.; Joos-Müller, B. *Adv. Polym. Sci.* **1998**, *136*, 139.
(28) Gohr, K.; Schartl, W. *Macromolecules* **2000**, *33*, 2129.
(29) Krom, J.; Wang, X. US Patent 6,437,050 B1, Aug 20, 2002.
(30) Funke, W. *J. Oil Col. Chem. Assoc.* **1977**, *60*, 438.
(31) Mallan, J. M.; Bebb, R. L. *Chem. Rev.* **1969**, *69*, 9.
(32) Payne, A. R. *J. Appl. Polym. Sci.* **1962**, *6*, 57.
(33) Payne, A. R.; Whittaker, R. E. *Rubber Chem. Technol.* **1971**, *44*, 440.
(34) Wang, M.-J. *Rubber Chem. Technol.* **1998**, *71*, 520.
(35) Bares, J. *Macromolecules* **1975**, *8*, 244.

MA048499V